ACS OMEGA

Open Access

http://pubs.acs.org/journal/acsodf

Article

Role of Alkannin in the Therapeutic Targeting of Protein-Tyrosine Phosphatase 1B and Aldose Reductase in Type 2 Diabetes: An *In Silico* and *In Vitro* Evaluation

Mohd Saeed, Ambreen Shoaib, Munazzah Tasleem, Asma Al-Shammary, Mohd Adnan Kausar, Zeina El Asmar, Abdelmuhsin Abdelgadir, Abdel Moneim E. Sulieman, Enas Haridy Ahmed, Maryam Zahin, and Irfan Ahmad Ansari*

Cite This: *ACS Omega* 2024, 9, 36099−36113

Read Online

ACCESS | Metrics & More | Article Recommendations | Supporting Information

ABSTRACT: Alkannin is a plant-derived naphthoquinone that is isolated from the Boraginaceae family plants. In our previous studies, we found that shikonin, which is the *R*-enantiomer of alkannin, has potent antidiabetic activity by inhibiting the action of the aldose reductase (AR) enzyme and the protein-tyrosine phosphatase 1B (PTP1B). Therefore, in this study, we aim to explore the antidiabetic effect of alkannin targeting PTP1B and AR by employing *in silico* and *in vitro* techniques. For *in silico*, we used different parameters such as ADMET analysis, molecular docking, MD simulation, Root Mean Square Deviation (RMSD), protein−ligand mapping, and free binding energy calculation. The *in vitro* evaluation was done by assessing the inhibitory activity and enzyme kinetics of PTP1B and AR inhibition by alkannin. The *in silico* studies indicate that alkannin possesses favorable pharmacological properties and possesses strong binding affinity for diabetes target proteins. Hydrogen bonds (Val297, Ala299, Leu300, and Ser302) and hydrophobic interactions (Trp20, Val47, Tyr48, Trp79, Trp111, Phe122, Trp219, Val297, Cys298, Ala299, Leu300, and Leu301) are established by the compound, which potentially improves specificity and aids in the stabilization of the protein−ligand complex. The results from *in vitro* studies show a potent dose-dependent PTP1B inhibitory activity with an IC_{50} value of 19.47 μM, and toward AR it was estimated at 22.77 μM. Thus, from the results it is concluded that a low IC_{50} value of alkannin for both PTP1B and AR along with favorable pharmacological properties and optimal intra-molecular interactions indicates its utilization as a potential drug candidate for the management of diabetes and its end complications.

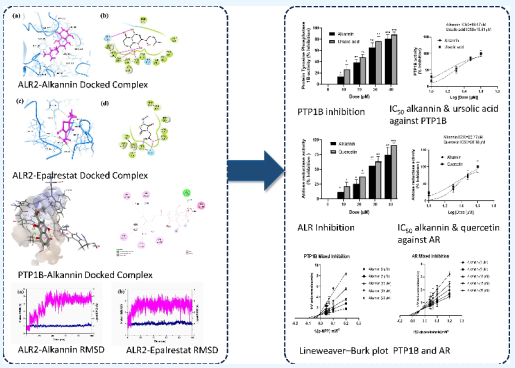

1. INTRODUCTION

Diabetes mellitus (DM) is regarded as one of the most frequent chronic ailments faced by humanity.[1] It is growing at an alarming rate and known to be a persistent reason for morbidity and mortality.[2] The disease as well as the economic burden of DM are not only debilitating but also devastating.[1,3] The WHO estimated that around 366 million people were suffering from diabetes in 2011, and this figure will drastically rise to 552 million by 2030.[4] The projected global incidence of diabetes in 2000 was 2.8%, and it is predicted to be 5.4% in 2025.[4] In terms of the incidence of DM, Saudi Arabia is ranked seventh in the world with an estimated 3.4 million cases. According to recent data, around 24.4% of adults living in Saudi Arabia are diabetic. There can also be seen a trend of ever-increasing rates of noncommunicable diseases.[5−7] There is an upsurge in the worldwide prevalence of noncommunicable as well as chronic illnesses at a frightening and disturbing rate. Each year nearly 18 million people die due to cardiovascular diseases; hypertension and diabetes are some of their foremost predisposing factors.[8] Driving this surge in cases related to hypertension as well as diabetes is the ever-increasing prevalence of obesity. These occur at an upsetting rate, joining with malnutrition and infectious diseases as the leading health-related problems wreaking havoc across the world.[9,10]

Insulin resistance, which occurs in conjunction with obesity and T2DM, is a pathophysiological condition characterized by abnormal cellular response to insulin.[11−13] Therefore, the liver's ability to produce glucose is reduced and there is no activation of GLUT-4-mediated glucose absorption, especially in peripheral tissues.[14] The liver plays a crucial role in regulating the metabolism of glucose and lipids throughout the body. It is believed that impaired insulin action in the liver is a

Received: January 3, 2024
Revised: July 22, 2024
Accepted: July 24, 2024
Published: August 18, 2024

main cause of insulin resistance, which requires higher levels of insulin in the bloodstream to effectively control blood glucose levels.[15−17] Insulin typically stimulates anabolic metabolism in the liver by enhancing glucose uptake and promoting lipid synthesis. In pathological conditions such as obesity and T2DM, insulin is unable to effectively control liver metabolism, resulting in excessive glucose production despite increased lipid synthesis (causing hyperglycemia and hypertriglyceridemia). This condition is commonly known as selective hepatic insulin resistance.[18] As a result, insulin-resistant illnesses, such as obesity and T2DM, are strongly associated with nonalcoholic fatty liver disease (NAFLD), a condition that can cause liver dysfunction and potentially develop into fatal nonalcoholic steatohepatitis.[19]

Alkannin is a plant-derived naphthoquinone that is isolated from the Boraginaceae family of plants.[20] Both the food coloring and cosmetic industries use dye. In nations like Australia and North India, it is used as a reddish-brown food additive.[20,21] Alkanet roots are utilized in a variety of ways for a variety of reasons. Naphthoquinone, alkannin, shikonin, and flavonoids are the active components found in alkanet roots. These substances all possess antiviral, anti-inflammatory, antibacterial, anticancer, antidiabetic, antiaging, antioxidant, and wound-healing characteristics. Skin conditions and wounds are treated with their roots.[22] Alkannin is a pigment that is deep red in an acidic environment and blue in an alkaline one.[23] Brockmann was the first to identify the chemical structure as a derivative of naphthoquinone. Shikonin, as the *R*-enantiomer of alkannin, has distinct stereochemical properties due to its unique chemical configuration, which contributes to its distinct pharmacological profile.[24] In our previous studies, it has been found that shikonin inhibits essential enzymes associated with diabetes, including aldose reductase (AR)[25] and the protein-tyrosine phosphatase 1B (PTP1B).[26]

Some of the enzymes that are very important in type 2 diabetes are PTP1B, glucokinase, dipeptidyl peptidase-IV, AR, etc. As a negative regulator, PTP1B is a unique enzyme, which is involved in insulin signaling pathways and is linked to T2DM and other metabolic diseases.[26] This works by lowering insulin resistance and bringing insulin and blood glucose levels back to normal without causing hypoglycemia.[26,27] AR, a NADPH-dependent oxidoreductase, catalyzes glucose to sorbitol in hyperglycemia and is a crucial enzyme of the polyol pathway, which takes a small quantity of nonphosphorylated glucose to metabolism. Sorbitol dehydrogenase converts sorbitol to fructose. Osmotic stress from sorbitol deposition and redox imbalance following NADPH depletion causes organ injury, cell damage, cataract formation, neuropathy, and other diabetes consequences. Thus, AR inhibition is a key method for preventing and reducing long-term diabetic problems.[25,28] Thus, in light of this, the purpose of this research was to discover new leads about the inhibition of PTP1B and AR by alkannin for the treatment of diabetes mellitus.

2. MATERIALS AND METHODOLOGY

2.1. Chemicals and Reagents. Alkannin (purity ≥98%) was procured from Cayman. DL-Glyceraldehyde, quercetin (purity ≥95%), nicotinamide adenine dinucleotide phosphate (NADPH), pNPP, metformin (purity ≥97%), and DMSO were obtained from Sigma-Aldrich. PTP1B (human recombinant) (purity ≥90%) was procured from Biomol. Recombinant human aldose reductase (purity ≥95%) was purchased from BioVision Inc., USA. FBS, MEM, antibiotic−antimycotic solution, and other tissue culture chemicals were purchased from Gibco. The fluorescent D-glucose analogue 2-[*N*-(7-nitrobenz-2-oxa-1,3-diazol-4-yl) amino]-2-deoxy-D-glucose (2-NBDG) was purchased from Life Technologies. Human insulin was obtained from Eli Lilly.

2.2. ADMET Analysis. The alkannin compound was obtained from PubChem as a three-dimensional structure in the form of "sdf" file format[29] and was subjected to drug-likeness evaluation by employing various modules of Discovery Studio (DS) [Dassault Systems, BIOVIA Corp., San Diego, CA, USA, v 21.1]. The structure was evaluated for drug-likeness using Discovery Studio (DS) [Dassault Systems, BIOVIA Corp., San Diego, CA, USA, v 21.1]. The ADMET and drug-likeness properties of alkannin were checked using the DS modules "Lipinski rule of 5", "ADME", and "TOPKAT".[30,31]

2.3. Docking and Interaction Studies. A technique called "molecular docking" uses the atomic-level interactions between small molecules and protein receptors. Alkannin compound was prepared for docking by employing the Prepare Ligand module from DS [Dassault Systems, BIOVIA Corp., San Diego, CA, USA, v 21.1]. The three-dimensional structure of PTP1B (PDB ID: 1AAX_A) was downloaded from the RSCB protein data bank (http://www.rcsb.org/).[32] It comprises 321 amino acids and was solved by X-ray crystallography. Water molecules and cocrystal ligands were removed from the protein. The binding sphere of radius 10 Å and *x*, *y*, and *z* coordinates 10.1919, 0.875726, and 11.2588, respectively, was created around the cocrystal ligand in the binding pocket. The AR (PDB ID: 4JIR_A), consisting of 316 amino acid residues bound with an inhibitor epalrestat was retrieved from RCSB.[33] The inhibitor was removed from the binding pocket, and a sphere of radius 6.16 Å at *x*, *y*, and *z* coordinates of −6.006635, 8.699351, and 17.461082, respectively, was created around it. Docking of protein structures with the alkannin was carried out by the CDocker module from DS. The "View Interaction" module was utilized to visualize the intramolecular interaction of the best-docked pose showing the highest CDocker score.

2.4. MD Simulation Studies. We conducted Molecular Dynamics (MD) simulations to investigate the dynamic stability and molecular interactions of alkannin when bound to the active site of the aldolase reductase. We placed each molecule complex in an orthorhombic simulation box measuring 10 Å in each dimension, filled with an explicit TIP4P water model, using the free academic Desmond-Maestro interpolarity tool. We added 0.15 M of either Cl^- or Na^+ ions to the system to neutralize it and mimic biological circumstances. We used Desmond's default minimization parameters to minimize the energy of each complex after the system was ready. Subsequently, each complex (alkannin and epalrestat) underwent a 100 ns MD simulation, recorded in 5000 frames, under conditions of 1.01325 bar pressure and a temperature of 300 K, using the standard parameters of the Desmond 2020−4 system. The resulting data, including the root mean square deviation (RMSD) values of the α carbon of the protein backbone and the ligand-fitted protein, RSMSF values, and protein−ligand contact graph, were plotted using the simulation interaction diagram tool.

2.5. Molecular Mechanics Generalized Born Surface Area (MM/GBSA) Calculations. The final binding free energy of each molecular complex was determined by

https://doi.org/10.1021/acsomega.4c00082
ACS Omega 2024, 9, 36099−36113

analyzing the last ten configurations from the molecular dynamics (MD) simulation trajectories. These configurations were processed using the Prime MMGBSA module of the Schrödinger suite, in accordance with the previously established MMGBSA methodology. In line with prior research,[34,35] the trajectories were adjusted by removing the explicit TIP4P water molecules and ions, ensuring a more refined analysis of the molecular interactions.[36]

2.6. Determination of PTP1B Activity. PTP1B inhibitory activity was estimated using pNPP as described elsewhere.[37] Recombinant PTP1B enzyme (0.5 units diluted in PTP1B reaction buffer) was added to a plate with or without alkannin. The plate was preincubated at 37 °C for 10 min, and then substrate (2 mM pNPP) was added. Following incubation at 37 °C for 15 min, the enzymatic reaction was terminated by the addition of 10 M NaOH. The absorbance was measured at 405 nm by using a microplate reader. Ursolic acid was used as a reference compound.

2.7. Determination of AR Activity. Recombinant human AR activity was assayed spectrophotometrically by measuring the decrease in absorption of NADPH at 340 nm over a 4 min period with DL-glyceraldehyde as a substrate.[38] Each 1.0 mL cuvette contained equal units of enzyme, 0.05 M sodium phosphate buffer (pH 6.2), and 0.3 mM NADPH with or without 10 mM substrate and alkannin. For inhibition studies, a concentrated stock of alkanin prepared in DMSO was used. Quercetin was used as a reference compound.

2.8. Kinetic Study. In order to determine the kinetic mechanism, the Lineweaver−Burk plot (double reciprocal plot), for PTP1B and AR, was obtained in the presence of various concentrations of alkannin (0, 5, 10, 15, and 20 μM). The type of inhibition was determined by observing a double reciprocal plot.

2.9. Cell Culture, Insulin Resistance Induction, and Glucose Uptake Assay. HepG2 liver cells were procured from ATCC (HB-8065). HepG2 cells were routinely grown in MEM supplemented with 10% (v/v) FBS, 1% antibiotic−antimycotic solution, in a humidified atmosphere of 95% air containing 5% CO_2 at 37 °C.

MTT assay was performed as described previously by Xu et al.[39] Briefly, HepG2 cells were seeded onto 96-well plates at a density of 5×10^3 cells/well for 24 h. Then the cells were treated with various doses of alkannin dissolved in DMSO. After another 24 h of incubation, the MTT was added, and later the absorbance of each well was recorded to calculate cell viability.[39]

The establishment of an insulin-resistant HepG2 (IR-HepG2) cell model and glucose uptake were performed according to Liu et al.[40] Briefly, HepG2 cells (5×10^3) were grown in a 96-well plate. After the confluence was reached, the cells were treated with insulin (1 μM) for 24 h to induce insulin resistance. These IR-HepG2 cells were further treated with different concentrations of alkannin for 24 h, followed by incubation with insulin (1 μM) for 30 min. Subsequently, 2-NBDG uptake in IR-HepG2 cells was measured. The cells were incubated with 50 μM 2-NBDG for 30 min.[40−43] Later, the cells were washed with ice-cold PBS, and the fluorescence intensity of 2-NBDG was measured on a Synergy HT microplate reader at 485 nm excitation and 528 nm emission.

2.10. Real-Time Quantitative RT-PCR. HepG2 cells (1×10^6) were grown in a 25 cm^2 flask for 24 h, followed by exposure to different concentrations of alkannin for 24 h, along with an untreated control. After treatment, total RNA was extracted by a PureLink RNA extraction Mini Kit. A Nanodrop spectrophotometer was used to estimate the quantity and quality of extracted RNA. Subsequently, Verso cDNA synthesis was used to synthesize first strand cDNA using 2 μg of total RNA, and NCBI primer pick was used to design the primer sequence for the target gene. Lastly, real-time PCR was performed by using a DyNAmoColorflash SYBR Green qPCR kit as per the manufacturer instruction. PTP1B gene was amplified by real-time PCR using standard protocols. The ΔΔCt method was used to calculate fold change in the gene expression. GAPDH gene was used as an internal control.

Primer for PTP1B: Forward primer (5′to 3′): TGTC-TGGCTGATACCTGCCTCT Reverse primer (5′to 3′): ATCAGCCCCATCCGAAACTTCC

2.11. Statistical Analysis. All the results shown in the study are mean ± SEM. The statistical significance was calculated by One-way ANOVA (GraphPad Prism 8.0). A p-value <0.05 was considered significant.

3. RESULTS

3.1. ADMET Analysis. The molecular weight of alkannin ranges between 297 and 404 Da. There are no functional groups that are toxic in alkannin. Log S levels of alkannin are within the permissible range for 95% of the currently available medications. Alkannin's general pharmacological traits (Tables 1 and 2) demonstrate that the molecule is biologically active and devoid of toxic functional groups. ADME-plot is a 2D plot that employs the calculated PSA_2D and Alogp98 properties. Figure 1 displays the graph depicting the relationship between Alogp98 and PSA. In the BBB plot, alkannin falls outside the 95% ellipse; however, it falls within 99% ellipse, showing BBB penetration. Alkannin was observed to possess poor aqueous solubility. Importantly, alkannin is not an inhibitor of cytochrome P450 2D6.

Table 1. Comprehensive ADMET Profiling of Alkannin: Elucidating the Pharmacokinetic and Safety Characteristics of Alkannin

ADMET Parameter	Values
Solubility	3
AlogP98	0
BBB	3
CYP2D6	FALSE
Hepatotoxic	TRUE
Absorption	0
PPB	TRUE
PSA 2D	97.048
Molecular Weight	288.295
Hydrogen bond Donors	3
Hydrogen bond Acceptors	5
Rotatable Bonds	3
Rings	2
Aromatic Rings	1

TOPKAT in DS predicts different toxicity parameters, namely, rodent carcinogenicity, rat oral LD50, Ames mutagenicity, DTP, and skin sensitization, based on the chemical structure of compounds. Various calculated parameters for alkannin are tabulated in Table 2. Models that satisfy each validation requirement for each query compound are calculated. The outcomes for each parameter were recorded. Though the compound showed hepatotoxicity, it was found to

https://doi.org/10.1021/acsomega.4c00082
ACS Omega 2024, 9, 36099−36113

Table 2. Predictive Toxicology Evaluation of Alkannin Using TOPKAT: Computational Analysis Elucidates Potential Toxicological Traits

Toxicity Parameters[a]	Prediction
Mouse NTP (F)	NC
Mouse NTP (M)	NC
Rat NTP (F)	NC
Rat NTP (M)	NC
Mouse Female	NC
WOE	NC
Carcinogenic Potency TD50 Mouse	132.774 mg/kg_body_weight/day (mg/kg_body_weight/day)
Carcinogenic Potency TD50 Rat	25.17 mg/kg_body_weight/day
Ames Prediction	NM
DTP	Toxic
Rat Oral Median Lethal Dose (LD50)	1.33207 g/kg_body_weight
Rat Inhalation Median Lethal Concentration (LC50)	2359.66 mg/m3/h
Chronic LOAEL	0.0825521 g/kg_body_weight
Skin Irritancy	Non-irritant
Skin Sensitization	Strong
Ocular Irritancy	None
Biodegradability	Degradable
Fathead Minnow LC50	0.0185828 g/L
Daphnia EC50	25.4641 mg/L

[a]Note: NTP: National Toxicology Program, WOE: weight of evidence, DTP: developmental toxicity potential, F: female, M: male, NC: non-carcinogen, NM: non-mutagen.

be nonmutagen, noncarcinogen, with no ocular and skin irritation, and biodegradable.

3.2. Docking and Intramolecular Interaction. The molecular docking technique has been a significant step in discovering potential inhibitors or repurposing drugs against potential drug target proteins for various diseases. The main goal of molecular docking is to understand how well a ligand binds to a target protein and the nature of its intramolecular interactions. In the current study, the interaction of the alkannin compound and aldose reductase protein was analyzed by molecular docking. The aim of this study was to evaluate the inhibition potential and binding affinity of alkannin with aldose reductase. Docking results indicated that alkannin binds to the active site of the aldose reductase. The binding achieved a docking score of −8.1 kcal/mol. This demonstrates a strong binding affinity. Moreover, residues V297, A299, L300, and S302 were involved in the interaction of hydrogen bonding. On the other hand, residues like W20, V47, Y48, W79, W111, F122, W219, V297, C298, A299, L300, and L301 are hydrophobic in nature (Figure 2). In comparison with alkannin, the docking energy of the reference molecule (epalrestat) was −5.7 kcal/mol. However, several residues were involved with different interactions between protein and ligand during docking, and the intermolecular interaction analysis of the protein−ligand complex displayed the presence of two hydrogen bonds with residues Y48, H110, and W111. Also, hydrophobic interactions were shown by residues W20, V47, Y48, W79, W111, F121, F122, W219, C298, and L300. Polar bonds are also exhibited by H110 residue (Figure 2).

Figure 3 illustrates the interaction of alkannin within the binding pocket of PTP1B with a -CDOCKER score of 29.066. Alkannin forms hydrogen bonds with L300 and π-alkyl hydrophobic interactions with W20, H110, W111, W209, and C298. Additionally, it forms a $\pi-\pi$-stacked interaction with W219. The hydrogen bonds thus formed so far are

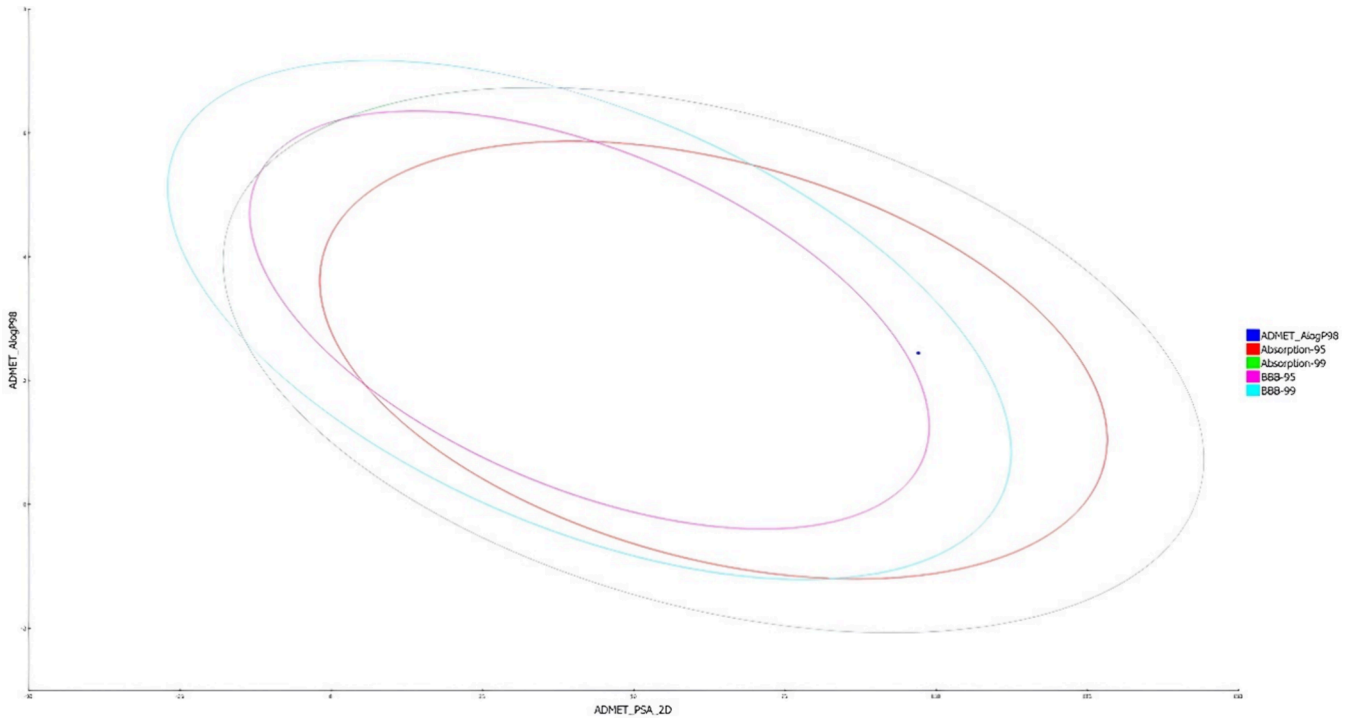

Figure 1. Pharmacokinetic parameters interact in the ADMET biplot curve, shown by the ellipses. These ellipses define BBB penetration and intestinal absorption predictive models. The representation allows compounds in these ellipses to be visually identified and assessed for brain permeability and gastrointestinal absorption.

https://doi.org/10.1021/acsomega.4c00082
ACS Omega 2024, 9, 36099−36113

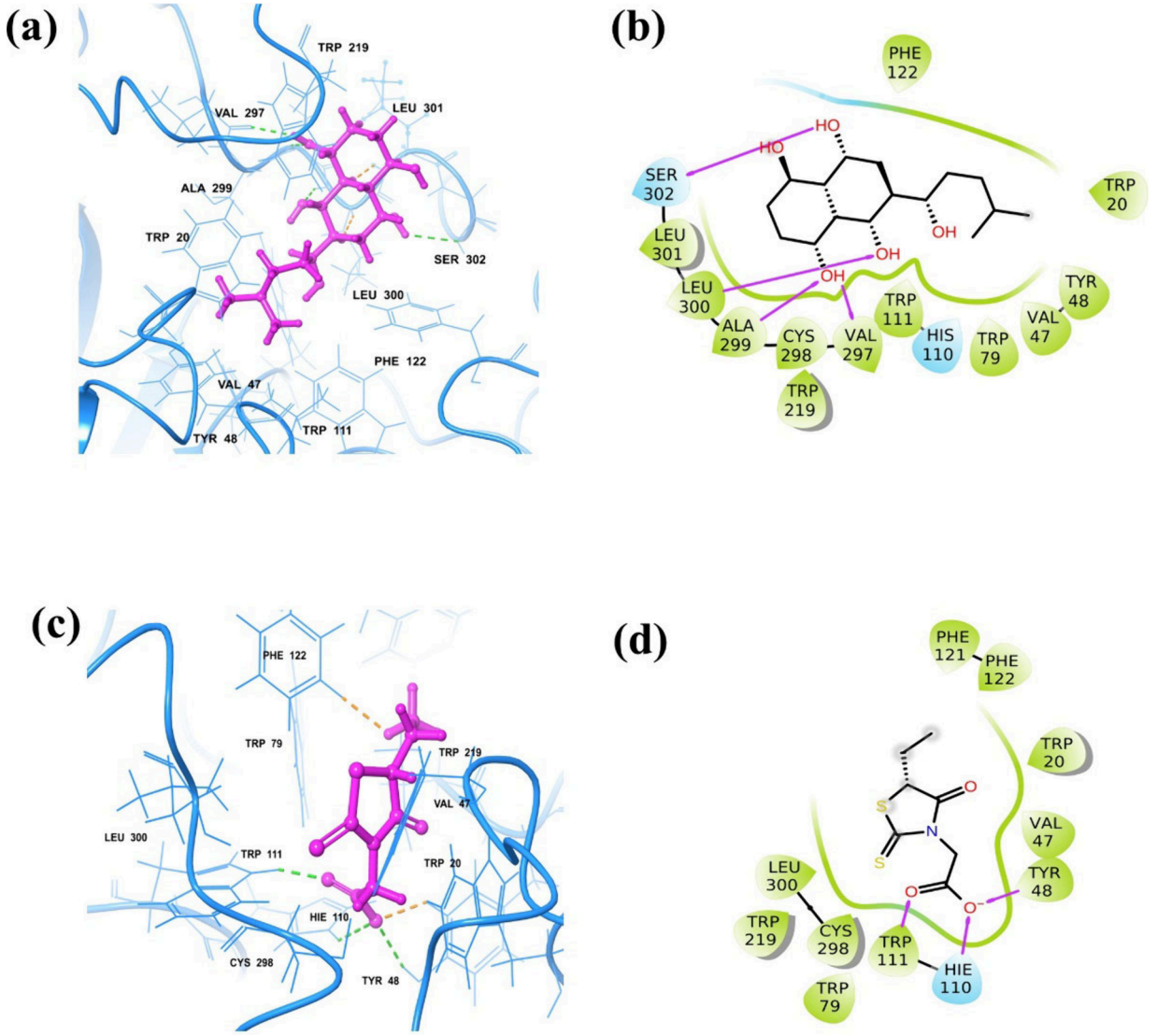

Figure 2. Visualization of molecular interactions: 3D and 2D interaction diagrams depicting the docked complex of aldose reductase with alkannin (A, B) and epalrestat (C, D).

stabilizing the complex formation, however, the hydrophobic interactions are required for the specificity of the ligand binding.[44]

3.3. MD Simulation. Molecular dynamics simulation helps us to understand the stability of docked complexes and study the interactions involved during the binding of ligands to proteins with respect to time. Herein, the last pose of the docked complex was retrieved from the 100 ns simulation trajectory to study the intramolecular interaction of the protein−ligand complex. Remarkably, the last pose of the complex also displayed a significant number of hydrogen bond formations with C298, A299, L300, L301, and S302 (Figure 4). This interaction study suggests that the last pose has some common interaction residues, as in the docked complex. Also, the residues of epalrestat molecule Y48 and W111 continued to form hydrogen bonds, which shows similar interactions as docking, which shows a stable interaction within the residues as depicted in Figure 4. This observation finalizes the stability of the ligand in the active site of the aldose reductase protein. Further analysis was carried out by RMSD, RMSF, and Protein−ligand interaction profiling studies.

3.4. Root Mean Square Deviation (RMSD). The concept of RMSD is integral in understanding the variance over time in the α carbon of a protein and the atoms within a ligand. During the analysis of a protein−ligand complex, particularly one involving an inhibitor, it is noted that the protein maintains a commendable level of stability, with deviations remaining below 1 Å throughout the simulation duration. Conversely, the alkannin presents more dynamic behavior. Initially, within the first 30 ns, it experiences a fluctuation of up to 4 Å. Post this period, there is a notable shift in its behavior, with deviations oscillating between 4 and 6 Å. In comparison, the Epalrestat molecule maintains a consistent 3 Å deviation in its interaction with the protein, which itself shows a steady RMSD of 1 Å, as illustrated in Figure 5.

3.5. Root Mean Square Fluctuation (RMSF). The RMSF of the protein and ligand was also analyzed. The protein RMSF showed stability (2.4 Å) to 350 residues, and a higher peak was observed between 100 and 150 residue indexes before attaining stability. Each peak indicates the area or residues of protein that fluctuate during the simulation. The RMSF of protein in

https://doi.org/10.1021/acsomega.4c00082
ACS Omega 2024, 9, 36099−36113

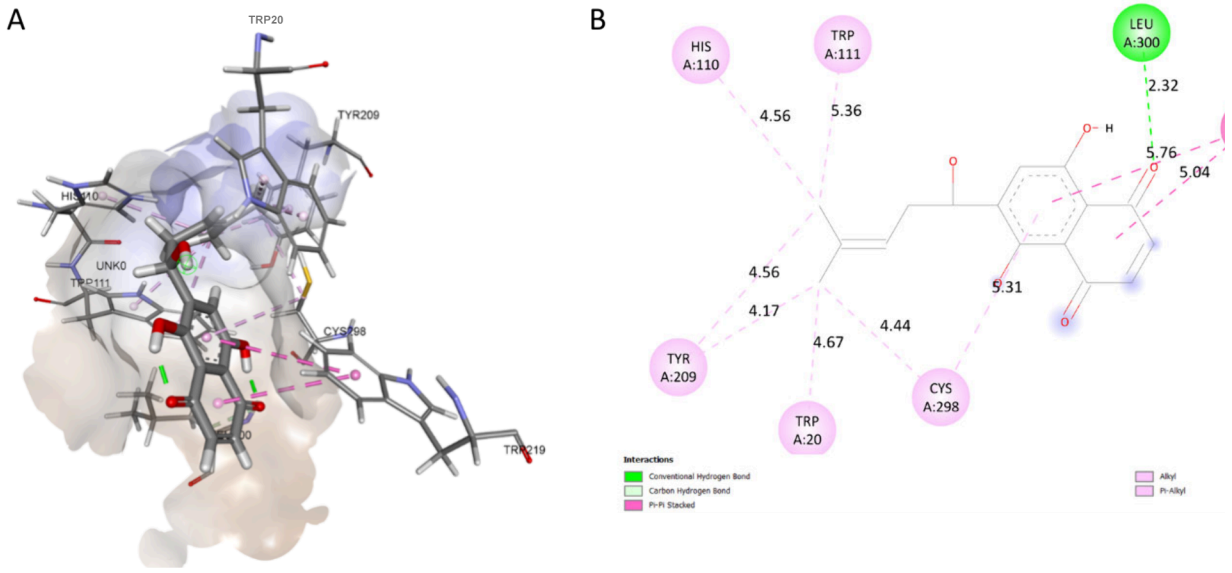

Figure 3. Visualization of alkannin interaction with PTP1B (PDB ID: 1AAX): (A) three-dimensional (3D) perspective and (B) two-dimensional (2D) representation. Hydrogen bonds are shown in green, and hydrophobic interactions are marked in pink. Distances between interactions are labeled in angstroms (Å), illustrating the molecular interactions between alkannin and PTP1B.

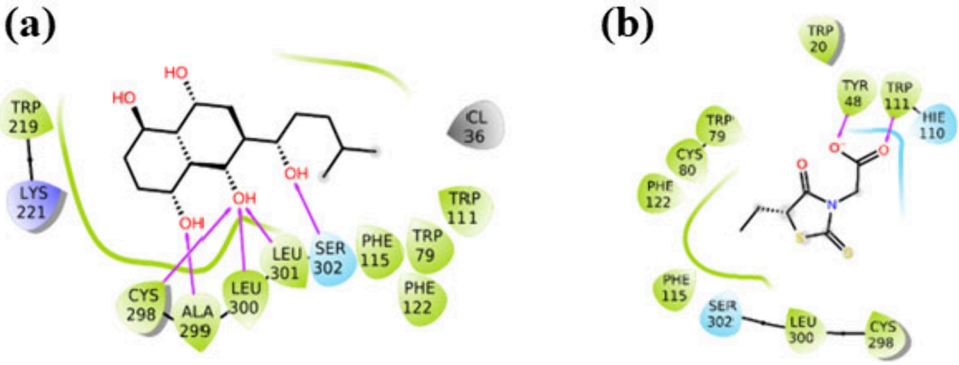

Figure 4. Concluding interaction profile: molecular docking complex of aldose reductase with (A) alkannin and (B) epalrestat, highlighting last-pose interactions.

the epalrestat molecule fluctuated to 2 Å during the simulation which is similar to the alkannin RMSF (Figure 6).

RMSF analysis of ligands showed acceptable fluctuations of atoms to (2 Å) in the alkannin RMSF. However, in the case of the epalrestat molecule, the ligand RMSF has been observed to have 1.5 Å. This finding supports that the selected ligand remains in the active site of the target protein (Figure 7).

3.6. Protein−Ligand Mapping. The protein−ligand interaction profiling was monitored throughout the simulation. The interaction profiling or contacts are studied based on four major contacts: Hydrogen bond, hydrophobic bond, ionic bond, and water bridge formation. The docked protein−ligand complex shows hydrogen bond formation with residues A299, L300, L301, and S302 for more than 40%−60% of the total simulation time, while W219 exhibits hydrophobic bond formation for more than 40% of the simulation time. R296 is involved in water bridge formation for more than 40% of the total interaction fraction. Additionally, the schematic diagram of ligand−protein contact also proves the involvement of R296 and A299 in hydrogen bond formation along with water molecules for more than 30% of the simulation time (Figures 8 and 9).

3.7. Free Binding Energy Calculation. In the evaluation of the binding free energy (ΔG) through the MM/GBSA method, a more accurate and repeatable assessment was achieved by integrating a range of physical and chemical factors. This process aids in identifying the most stable conformation, marked by the lowest possible energy. The ΔG binding free energy was determined from the last 10 ns of each trajectory, which encompassed 500 frames (Figure 10 and Table 3). This suggests that there was a 20 ps evaluation of the energy. Furthermore, the standard deviation of the binding free energy fluctuation was also calculated for the final 10 ns of the simulated pathway. The protein−ligand complex was examined for ΔG binding free energy after it was generated from a MD simulation. The results of this research showed that the protein−ligand combination had an energy level of −142.612 kcal/mol, which was unusually low. The energy level of the protein−ligand complex of the reference molecule, epalrestat, was measured at −143.343 kcal/mol, which was noticeably higher than this. These findings indicate the potential efficacy of the alkannin. Furthermore, the analysis demonstrated minimal variation in the MMGBSA score for the protein−ligand complex, further corroborating the ligand's stable interaction with the protein.

https://doi.org/10.1021/acsomega.4c00082
ACS Omega 2024, 9, 36099−36113

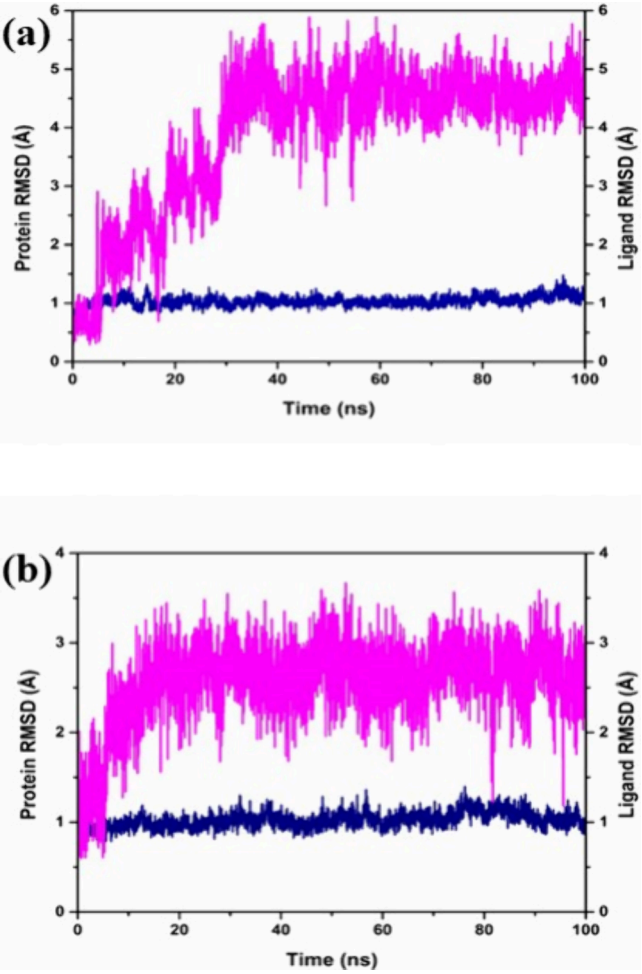

Figure 5. Root mean square deviation (RMSD) analysis: comparative plots for alkannin (A) and reference molecule (epalrestat) (B) over a 100 ns Molecular Dynamics (MD) simulation of the aldose reductase protein.

3.8. Inhibition of PTP1B and AR by Alkannin. The potential of alkannin against PTP1B was evaluated using *p*-nitrophenyl phosphate (pNPP) as a substrate. Alkannin showed strong inhibition of PTP1B with IC_{50} of 19.47 μM (Figure 11a,b). Ursolic acid, a positive control, showed inhibition of PTP1B with an IC_{50} of 15.81 μM (Figure 11a,b). Moreover, a concentration-dependent inhibition of PTP1B by alkannin was observed.

The effect of alkannin against AR was also determined, as shown in Figure 12. The IC_{50} value of alkannin against AR was found to be 22.77 μM (Figure 12a,b). Quercetin, a positive control, showed strong AR inhibition with an IC_{50} of 20.18 μM (Figure 12a,b). Moreover, a concentration-dependent inhibition of AR by alkannin was also observed. A low IC_{50} of alkannin for both PTP1B and AR indicates its utilization as a potential drug candidate.

3.9. Enzyme Kinetics of PTP1B and AR Inhibition by Alkannin. As shown in Figure 13a, alkannin exhibited mixed-inhibition against PTP1B. Similarly, data analysis from the Lineweaver−Burk plot indicated a mixed-inhibition of AR by alkannin (Figure 13b).

3.10. Effect of Alkannin on Glucose Uptake in Insulin-Resistant HepG2 Cells. Before determining the glucose uptake by IR-HepG2 cells in the presence of alkannin, the cytotoxicity of alkannin on normal HepG2 (N-HepG2) cells was determined by the MTT assay. HepG2 cells were pretreated with alkannin at concentrations up to 100 μM, following an incubation of 24 h. Alkannin exerted insignificant cytotoxicity up to 50 μM (Supplementary Figure S1), so doses lower than 50 μM were used in subsequent glucose uptake assay.

2-NBDG test was used to determine the glucose uptake in IR-HepG2 cells. Treatment of HepG2 cells with a high dose of insulin led to insulin-resistance, as indicated by the significant decline in glucose uptake in IR-HepG2 cells (Figure 14). N-HepG2 cells are normal untreated cells and there was no treatment of insulin on this group. The glucose uptake in these cells takes place normally, as occurs when cells are grown in an *in vitro* medium irrespective of stimulation of insulin. However, insulin resistant cells (IR-HepG2 cells) show reduced glucose uptake. That is why glucose uptake in N-HepG2 cells was kept 100% or in another word this group was set as control and glucose uptake in IR-HepG2 cells were reported relative to control. According to results, alkannin significantly enhanced insulin-stimulated 2-NBDG uptake in IR-HepG2 cells in a concentration-dependent manner. Thus, the result suggests that alkannin was able to induce insulin-sensitivity in IR-HepG2 cells, which was evident by the increased relative percentage of glucose uptake equivalent to metformin.

3.11. Effect of Alkannin on PTP1B mRNA Expression in IR-HepG2 Cells. PTP1B is a negative regulator of insulin signaling, and its overexpression is associated with insulin-resistance state. Accordingly, to confirm whether alkannin could increase insulin sensitivity of IR-HepG2 cells, we evaluated the mRNA expression of PTP1B in IR-HepG2 cells by qPCR analysis. PTP1B is known to be weakly expressed under normal glycemic conditions, while its expression is enhanced during an insulin-resistance state. Therefore, the decreased expression of PTP1B in IR-HepG2 cells could be an indication of insulin sensitizing properties. As can be seen in Figure 15, alkannin significantly reduced the PTP1B mRNA expression, revealing its insulin-sensitizing potential.

4. DISCUSSION

PTP1B has been recognized as an important therapeutic target for the management of T2DM. PTP1B plays a crucial role in the development of insulin resistance. Developing new inhibitors against PTP1B could lead to novel therapeutic approaches for the treatment of diabetes. These inhibitors can improve insulin sensitivity.[45,46] Moreover, AR, an important enzyme involved in diabetes end complications, is also considered to be a potential target to alleviate diabetes-associated disabilities. In this regard, plant-derived compounds could be more advantageous over synthesized compounds.[47]

In the current study, the role of alkannin, a bioactive compound of *Alkanna tinctoria*, against PTP1B and AR was investigated. Besides a good pharmacokinetic profile, alkannin has shown significant binding affinity with PTP1B and AR. Several factors are considered to consider a ligand as a therapeutic candidate. These factors include drug likeliness, molecular weight, logP, logS, and toxicity risks. These factors help assess the compound's overall potential. Alkannin appears to have a logP (octanol/water) value suitable for biological activity. Additionally, it has no toxic functional groups.[48] One of the important factors for the development of a drug compound is aqueous solubility, the alkannin was found to

https://doi.org/10.1021/acsomega.4c00082
ACS Omega 2024, 9, 36099−36113

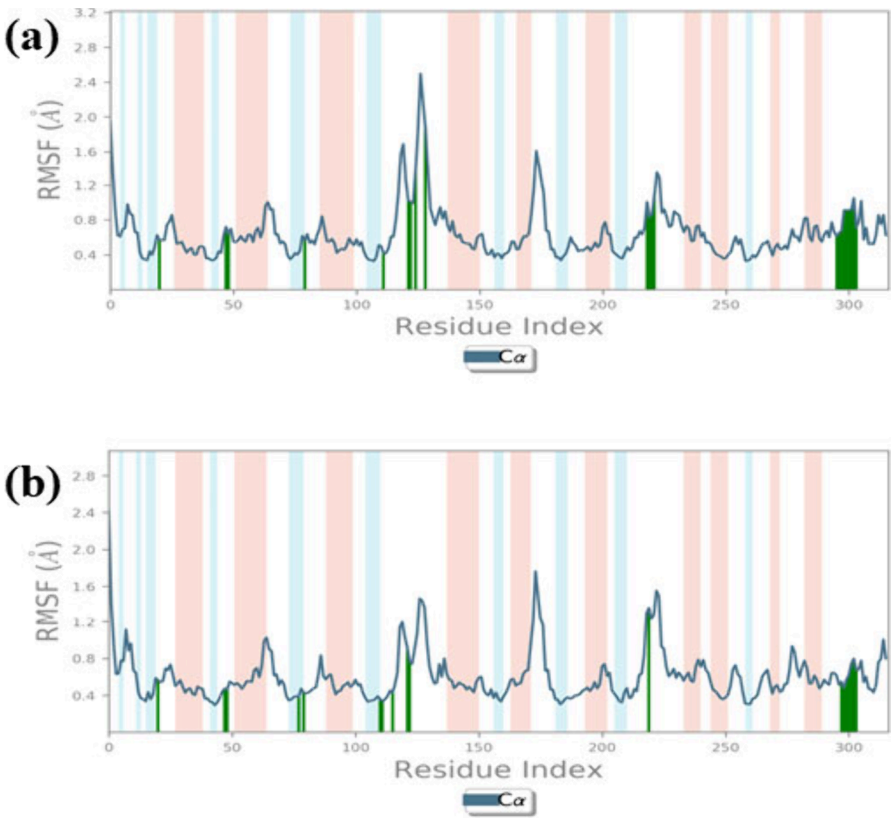

Figure 6. Comparison of protein RMSF profiles: alkannin (A) and reference molecule (epalrestat) (B) during a 100 ns MD simulation of aldose reductase.

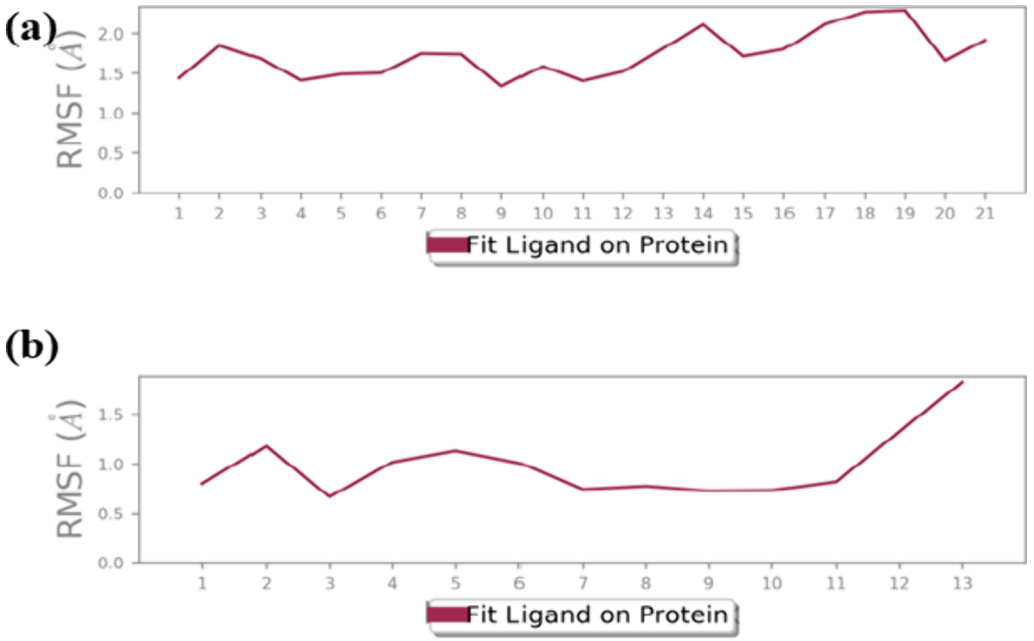

Figure 7. Ligand-specific RMSF profiles: comparative analysis of alkannin (A) and reference molecule (epalrestat) (B) during a 100 ns MD simulation of aldose reductase protein.

possess poor aqueous solubility; however, alkannin falls within 99% ellipse, represents good BBB penetration for higher efficacy.[49] The alkannin is not a CYP2D6 inhibitor; therefore, it will not lead to elevated levels of plasma concentration thereby reducing adverse outcomes. The toxicity profile of alkannin was evaluated to be acceptable. Molecular docking is an integral element of the drug design procedure, which is employed in this study to assess the binding ability of alkannin to the target proteins.[50] Both target proteins formed hydrogen bonds with active site residues. They also formed hydrophobic interactions with these residues. Hydrogen bonds are among the most significant types of molecular interactions in biology.

https://doi.org/10.1021/acsomega.4c00082
ACS Omega 2024, 9, 36099−36113

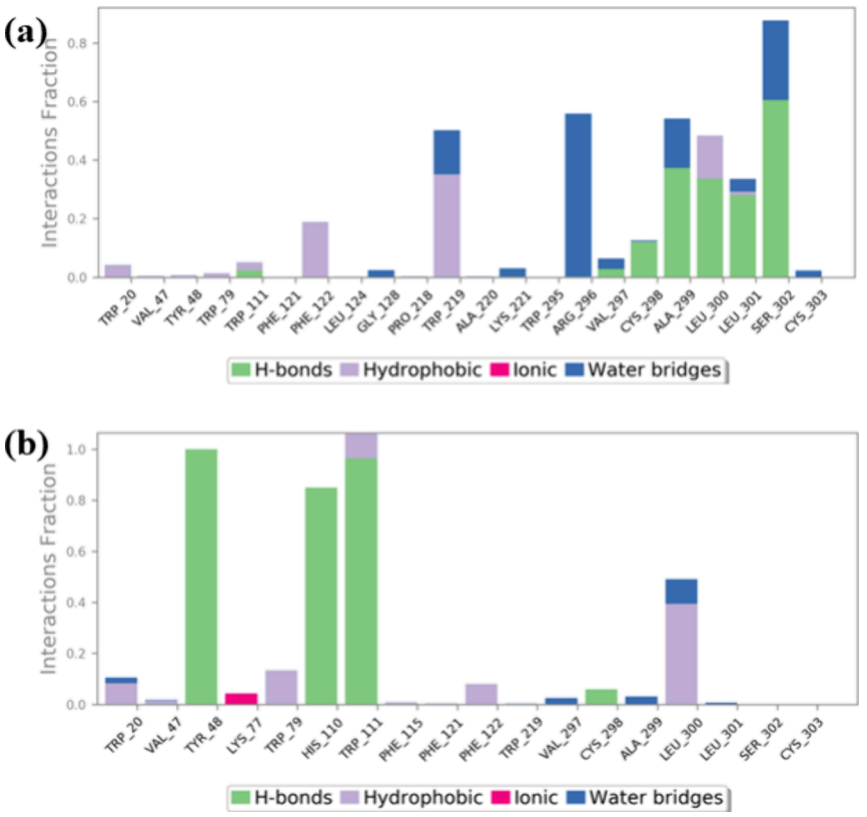

Figure 8. Comparing MD simulations of alkannin (A) and the reference molecule (epalrestat) (B) with aldose reductase protein to visualize protein−ligand interactions. The plots show the complex interactions between the ligands and the protein over a 100 ns simulation, revealing their binding modes and stability in the enzyme's active site.

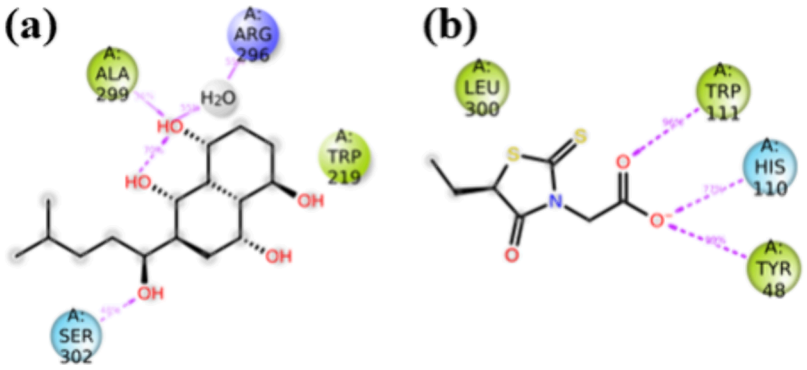

Figure 9. A 100 ns MD simulation of alkannin (a) and the reference molecule (epalrestat) (b) interacting with aldose reductase protein reveals ligand−protein contacts. The depiction shows the dynamic binding patterns and contact residues between the ligands and the protein's active site, revealing their molecular interactions and stability in the protein environment.

Through the encapsulation of hydrophobic groups and the exposure of hydrophilic groups, the hydrophobic effect provides a thermodynamic stimulus for nucleic acid structures, proteins, and membranes in water. Hydrogen bonds provide intramolecular interactions with directionality and specificity.[51] This study highlights the importance of alkannin as a possible inhibitor for aldose reductase through the investigation of molecular docking and dynamic simulations. The effectiveness of these inhibitors is critical in the field of medicine research and repurposing to fight a variety of illnesses. Alkannin's binding affinity to aldose reductase, as shown by a docking score of −8.1 kcal/mol, appears promising, according to the molecular docking analysis.[52] The hydrophobic properties of residues like W20, V47, Y48, and others, as well as the interactions of residues like V297, A299, L300, and S302 through hydrogen bonding, further confirm this. In comparison, the reference molecule epalrestat had a docking energy of −5.7 kcal/mol, which was lower. Nevertheless, it demonstrated a variety of interactions between residues, such as the creation of hydrogen bonds with Y48, H110, and W111, as well as hydrophobic interactions with a number of residues. These results highlight the subtle variations in each molecule's interactions with the target protein.

Additional insights are obtained from the molecular dynamic simulation, particularly from the examination of the docked complex's final position. The potential of alkannin as a stable inhibitor is highlighted by the regularity with which hydrogen bonds are formed with particular residues and the stability of

https://doi.org/10.1021/acsomega.4c00082
ACS Omega 2024, 9, 36099−36113

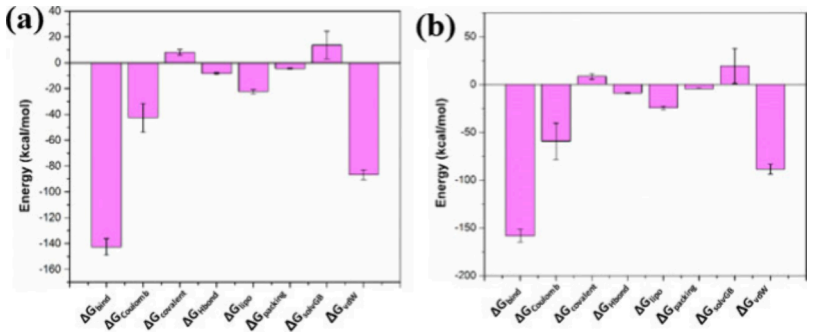

Figure 10. Comparative plotting of alkannin (a) and reference molecule (epalrestat) (b) after 100 ns MD simulation with aldose reductase protein. The MM-GBSA calculations show alkannin and epalrestat's energetic contributions and stability in the protein's active site, assessing their affinities and inhibitor potential.

Table 3. Binding Free Energy Calculation of Inhibitor and Control Docked Complexes

MM/GBSA Components	4JIR_ Alkannin	4JIR_ Epalrestat
ΔG_{Bind}	−142.61 ± 6.40	−158.33 ± 6.61
$\Delta G_{\text{Bind Coulomb}}$	−42.54 ± 11.16	−59.41 ± 18.79
$\Delta G_{\text{Bind Covalent}}$	8.09 ± 2.24	8.45 ± 3.02
$\Delta G_{\text{Bind Hbond}}$	−8.42 ± 0.75	−8.94 ± 0.52
$\Delta G_{\text{Bind Lipo}}$	−22.36 ± 1.54	−24.41 ± 1.83
$\Delta G_{\text{Bind Packing}}$	−4.41 ± 0.34	−4.47 ± 0.23
$\Delta G_{\text{Bind Solv GB}}$	13.72 ± 10.62	19.24 ± 18.44
$\Delta G_{\text{Bind vdW}}$	−86.67 ± 3.81	−88.78 ± 5.17

these interactions.[53] Hydrophobic interactions have a significant influence on the stability of a compound-protein interaction. These interactions promote stability by creating a hydrophobic environment with nonpolar regions of the compound and protein.[36] However, specific and directional hydrogen bond interactions contribute to the strength and specificity of a compound-protein interaction. Their presence is critical for keeping the complex in a stable and specific conformation.[37] Fluctuations in the region where these interactions are found indicate dynamic changes in the strength or geometry of these bonds. Such fluctuations can have an impact on the overall stability and conformation of the compound-protein complex.[38,39] Evaluating the stability of protein−ligand complexes involves several measurements. RMSD and RMSF measurements provide a thorough perspective on this stability. In contrast to epalrestat's more consistent pattern, alkannin's varying RMSD values indicate a dynamic interaction between alkannin and the protein. In the meantime, the simulation's regions of stability and variation in the protein structure are reflected in the RMSF study. The intricacy of these interactions is further explored by protein−ligand mapping. The complexity of molecular interactions is highlighted by the occurrence of hydrogen bonds, hydrophobic bonds, and water bridge forms at different points during the simulation. Last but not least, the MM/GBSA method's computation of free binding energy provides yet another level of insight. When compared to that of epalrestat, the lower energy levels for the alkannin complex indicate a stronger and more stable connection, suggesting the possible inhibitory efficacy of alkannin. Together, these thorough analyses offer a profound comprehension of the molecular interactions involved, opening the door for additional research in the field of drug development.

In the *in vitro* experiment, alkannin was found to strongly inhibit both PTP1B and AR enzymes, which was equivalent to reference molecules. Additionally, alkannin showed mixed-type inhibition of PTP1B and AR in enzyme kinetics study, substantiating that alkannin could bind to to the active sites as well as other allosteric sites of each enzyme. Regarding the rationale to select the doses of alkannin for further experiments, cell viability assay was used against HepG2 cells to observe whether alkannin is cytotoxic to these cells. We observed that alkannin was safe up to a 50 μM dose (Supplementary Figure S1). Therefore, we selected doses of alkannin below 50 μM. Recently Xue et al. reported the alkannin was playing protective role in HepG2 cells up to 40 μM when pretreated with palmitic acid. To date, the

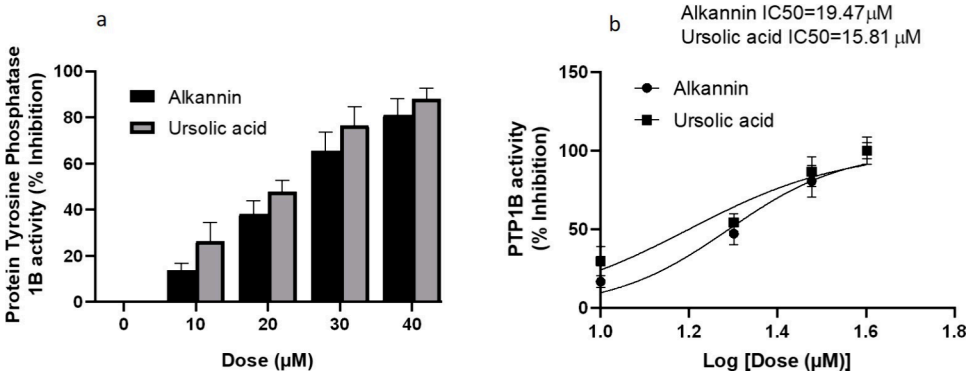

Figure 11. (A) Alkannin-mediated PTP1B inhibition. (B) IC_{50} graph of alkannin and ursolic acid against PTP1B. The data shown are the mean ± SEM of triplicate experiments (*p < 0.05, **p < 0.01, and ***p < 0.001 were considered significant as compared to control).

https://doi.org/10.1021/acsomega.4c00082
ACS Omega 2024, 9, 36099−36113

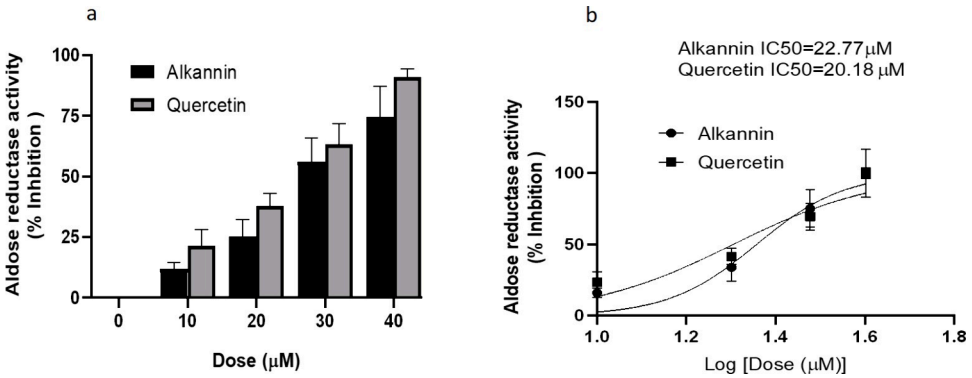

Figure 12. (A) Alkannin-mediated inhibition of AR enzyme (B) IC_{50} graph of alkannin and quercetin against AR. Data shown are mean ± SEM of triplicate experiments (*p < 0.05, **p < 0.01, ***p < 0.001 were considered significant as compared to control).

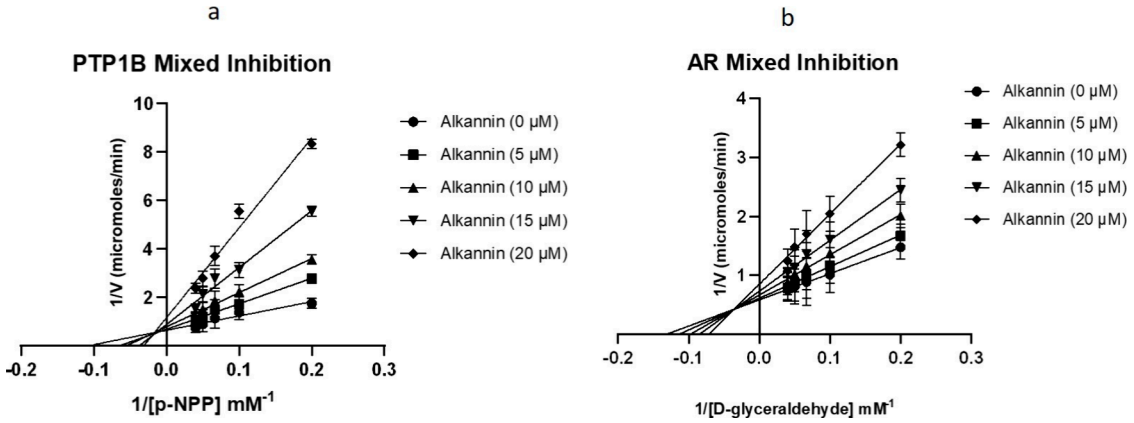

Figure 13. Lineweaver−Burk plot (A) for PTP1B and (B) for AR. Enzyme kinetics were studied in the presence of various concentrations of alkannin. Data shown are mean ± SEM of triplicate experiments.

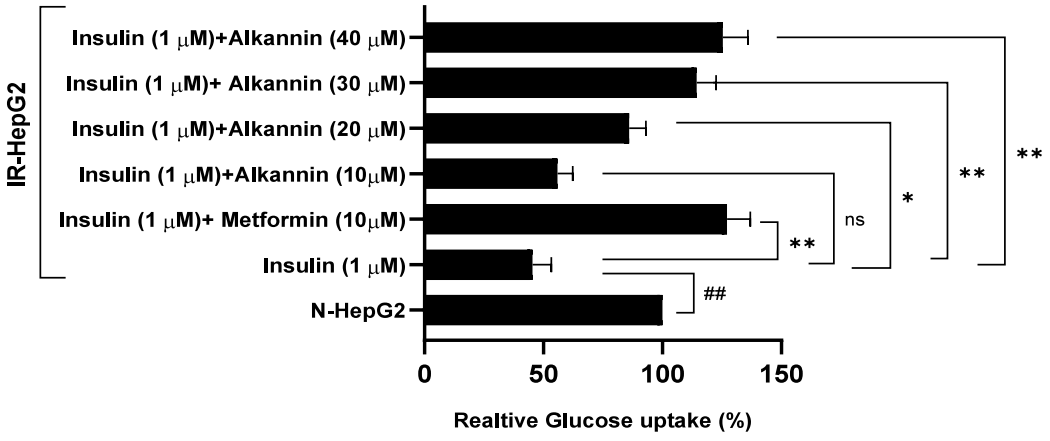

Figure 14. Effect of alkannin on insulin-stimulated glucose uptake in IR-HepG2 cells, as measured by the 2-NBDG method. Data shown are mean ± SEM of triplicate experiments. ###p < 0.001 indicates significant difference from the untreated normal control group; *p < 0.05, **p < 0.01, and ***p < 0.001 indicate significant difference from the insulin-resistant control group.

antidiabetic potential of alkannin has not been explored much. Moreover, most of the study of alkannin published is *in vitro*, i.e., on the cell line system. Additionally, no study to date has reported the detailed pharmacokinetics and bioavailability of alkannin. However, recently, alkannin has been shown to play a protective role in liver injury and inflammation in diabetic mice.[39] The C57BL/KsJ-db/db mice were given alkannin at doses of 20 and 40 mg/kg body weight, and alkannin was found to play a protective role. In light of the above, it can be concluded that the concentration reported in this study could be achievable in diabetic mice. However, further research is warranted to establish the therapeutic dose.

PTP1B is a negative regulator of the insulin signaling, and its level is increased during insulin-resistance.[46] Alkannin was found to stimulate glucose uptake in IR-HepG2 cells, which signified the improvement in insulin sensitivity in HepG2 cells. Similarly, in quantitative real-time PCR analysis, alkannin was also demonstrated to reduce the PTP1B mRNA expression in

https://doi.org/10.1021/acsomega.4c00082
ACS Omega 2024, 9, 36099−36113

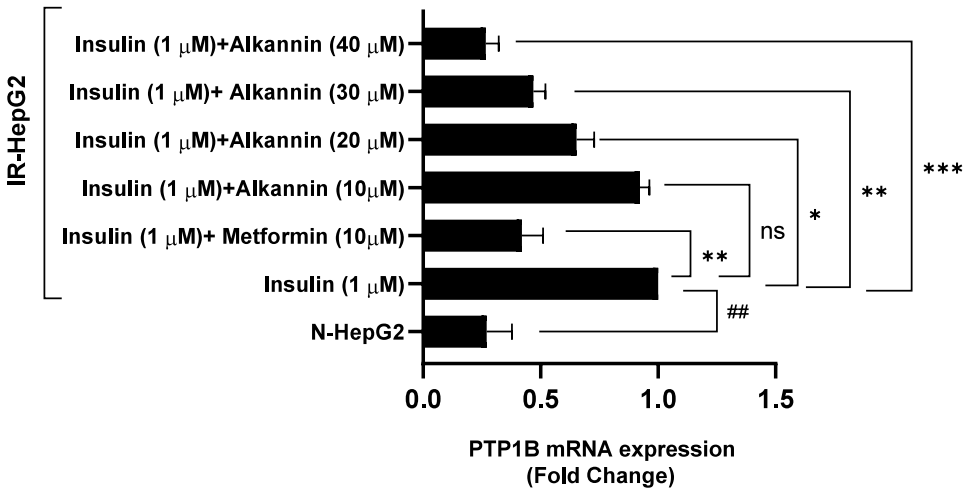

Figure 15. Effect of alkannin on PTP1B mRNA expression in IR-HepG2 cells. Data shown are mean ± SEM of triplicate experiments. $^{\#\#\#}p < 0.001$ indicates significant difference from the untreated normal control group; $^{*}p < 0.05$, $^{**}p < 0.01$ and *** $p < 0.001$ indicate significant difference from the insulin-resistant control group.

IR-HepG2 cells. Thus, our results revealed that alkannin could improve insulin sensitivity by reducing PTP1B expression. The outcome of the current study is in agreement with several previous reports where different plant products have been shown to stimulate insulin sensitization in the liver by improving insulin-resistance. For example, in a previous report, a flavonoid 7-*O*-methylaromadendrin, extracted from *Inula viscosa*, was demonstrated to enhance glucose uptake in IR-HepG2 cells. Moreover, it was found to improve insulin resistance in liver cells via activating PI3K and AMPK-dependent pathways.[43] In a similar study, a triterpenoid saponin isolated from *Stauntonia chinensis* was found to significantly stimulate glucose uptake in insulin-resistant HepG2 cells. Moreover, it was also shown to activate the insulin signaling in liver cells.[54] Similarly, cocoa polyphenolic extract and its major component (−)-epicatechin were found to ameliorate insulin-sensitivity of liver HepG2 cells under a high-glucose environment.[55] They potentially protect or delay hepatic dysfunction through the diminution of AMPK and PI3K/AKT insulin signaling blockade. In an interesting study, fumosorinone, a novel compound extracted from an insect fungi *Isaria fumosorosea*, was shown to exhibit potent PPTP1B inhibitory activity.[40] Moreover, it stimulated glucose uptake in IR-HepG2 cells. Similarly, fumosorinone was also found to decrease PTP1B in both IR-HepG2 cells and liver tissue of diabetic KKAy mice. Additionally, it was found to improve insulin sensitivity in the liver by triggering the insulin signaling pathway. In another study, bis (2, 3-dibromo-4, 5-dihydroxybenzyl) ether, extracted from a red alga *Odonthalia corymbifera*, was shown to be strong inhibitor of PTP1B.[39] Moreover, it was demonstrated to stimulate the glucose uptake in IR-HepG2 cells by activating the insulin signaling pathway. In a recent study, three major compounds from root bark of *Morus alba* such as mulberrofuran G, albanol B, and kuwanon G were found to potently inhibit PTP1B via mixed-type enzyme inhibition. Moreover, all the three compounds were found to enhance glucose uptake and reduce PTP1B expression in IR-HepG2 cells.[41] Overall, the above studies have corroborated our finding that alkannin could improve insulin-resistance by decreasing the expression of PTP1B in liver cells.

There is a long list of plant-derived chemicals that have been shown to exhibit AR inhibitory activities. Haragucci et al. demonstrated that 2,5-dihydroxy-*p*-benzoquinone, a derivative of *p*-benzoquinone, is a highly effective noncompetitive inhibitor of AR.[56] A recent study examined several naturally occurring quinones to determine their potential for inhibiting AR activity.[57] All quinones displayed notable inhibition against AR and demonstrated noncompetitive inhibition. Similarly, various flavonoids were found to inhibit the AR enzyme at micromolar doses.[58] Curcumin and its synthesized analogs were shown to exhibit in vitro AR inhibition. The IC_{50} of curcumin was found to be 6.8 μM, while that of analogs were in the range of 2.6−35.9 μM.[59] In another report, curcumin was also found to inhibit human recombinant AR in a noncompetitive manner.[60] Quercetin was shown to effectively inhibit AR in a noncompetitive manner, with a 95% inhibition observed at a dose of 10 μM. Additionally, it was found to effectively block the polyol pathway, as evidenced by an 80% reduction in the accumulation of xylitol.[61] In their study, Chaudhry et al. examined the effects of several flavonoids on human lens AR. They found that quercetin effectively inhibited AR by 50% when present at a dose of 5 μM.[62] Veverka et al. conducted a synthesis and screening of several acylated quercetin compounds. They found that the chloro-naphthoquinone derivative was the most effective in inhibiting AR.[63]

In a recent study, various 1,2-naphthoquinone derivatives were shown to exhibit submicromolar inhibition of PTP1B.[64] Moreover, nearly 500 natural compounds of different classes including phenols are comprehensively reviewed for their PTP1B inhibitory activity in a recent review.[65] The major groups of phenolics include α-pyrones, flavonoids, and phenolic acids. Coumarins are major representatives of alpha-pyrones, and many of them are reported to be PTP1B inhibitor. For example, two coumarins from *Artemisia capillaris* showed strong inhibition against PTP1B.[66] Six natural coumarin derivatives from *Angelica decursiva* were found significant PTP1B inhibitory.[67] A mixed-type PTP1B inhibitor was reported from *Euonymus alatus*.[68] Among flavonoids, more than 100 PTP1B inhibitors have been described. In a previous study, natural flavonoids extracted from the roots of the plant *Broussonetia papyrifera*, exhibited PTP1B inhibitory activity.[69] Similarly, quercetin-3-*O*-β-D-glucuronide and myricetin-3-*O*-β-

https://doi.org/10.1021/acsomega.4c00082
ACS Omega 2024, 9, 36099−36113

Dglucuronide, isolated from the leaves of *Cyclocarya paliurus*, showed significant PTP1B inhibitory activity (IC_{50} = 7.39 ± 1.15 μg/mL and 9.47 ± 3.31 μg/mL respectively).[70] Many other flavonols have been described to possess strong PTP1B inhibitory action.[71−74] A number of flavanones and isoflavones were also shown to have substantial PTP1B inhibitory action.[75−82] Chalcones have also been shown to exhibit noteworthy PTP1B inhibitory effect.[83−85] All of the above studies corroborate our finding that alkannin, being a natural naphthoquinone, has the potential to inhibit both PTP1B and AR activity.

5. CONCLUSION

In conclusion, the outcome of the study signifies the potential of alkannin in the therapeutic inhibition of PTP1B and AR via *in silico* and *in vitro* evaluation. Moreover, alkannin also increased the insulin sensitivity of insulin-resistant cells and enhanced the glucose uptake via PTP1B suppression, which substantiates the potential of alkannin to undergo further validation of its activities against various preclinical and clinical T2DM models. In addition, alkannin also inhibited the activity of AR *in vitro*, which indicated its drug-like potential and can be further tested in various diabetes-associated end complications like nephropathy and retinopathy models as well. Thus, the study provides scientific evidence supporting the pharmacological and therapeutic potential of alkannin for the management of type 2 diabetes. However, further in-depth investigations are required to establish the potential of alkannin for the management of T2DM.

■ ASSOCIATED CONTENT

Supporting Information

The Supporting Information is available free of charge at https://pubs.acs.org/doi/10.1021/acsomega.4c00082.

Figure S1: Percent cell viability of HepG2 cells after treatment with various doses of alkannin (10−100 μM) for 24 h (PDF)

■ AUTHOR INFORMATION

Corresponding Author

Irfan Ahmad Ansari − *Department of Biosciences, Integral University, Lucknow 226026, India;* orcid.org/0000-0002-9966-1225; Email: ahmadirfan.amu@gmail.com

Authors

Mohd Saeed − *Department of Biology, College of Sciences, University of Ha'il, Ha'il 81451, Saudi Arabia*

Ambreen Shoaib − *Department of Clinical Pharmacy, College of Pharmacy, Jazan University, Jazan 45142, Saudi Arabia*

Munazzah Tasleem − *Center for Global Health Research, Saveetha Medical College and Hospital, Chennai 602105, India*

Asma Al-Shammary − *Department of Public Health, College of Public Health and Health Informatics, University of Ha'il, Ha'il 81451, Saudi Arabia*

Mohd Adnan Kausar − *Department of Biochemistry, College of Medicine, University of Ha'il, Ha'il 81451, Saudi Arabia;* orcid.org/0000-0002-8931-9290

Zeina El Asmar − *Department of Biology, College of Sciences, University of Ha'il, Ha'il 81451, Saudi Arabia*

Abdelmuhsin Abdelgadir − *Department of Biology, College of Sciences, University of Ha'il, Ha'il 81451, Saudi Arabia*

Abdel Moneim E. Sulieman − *Department of Biology, College of Sciences, University of Ha'il, Ha'il 81451, Saudi Arabia;* orcid.org/0000-0002-9202-6624

Enas Haridy Ahmed − *University of Ha'il, Faculty of Medicine Anatomy Department, Ha'il, KSA, Ain Shams University, Faculty of Medicine Anatomy and Embryology Department, Cairo 11566, Egypt*

Maryam Zahin − *James Graham Brown Cancer Center, University of Louisville, Louisville, Kentucky 40202, United States*

Complete contact information is available at: https://pubs.acs.org/10.1021/acsomega.4c00082

Notes

The authors declare no competing financial interest.

■ ACKNOWLEDGMENTS

This research has been funded by Scientific Research Deanship at University of Ha'il - Saudi Arabia through project number RG-21 122

■ REFERENCES

(1) Shoaib, A. A Nanotechnology-Based Approach to Biosensor Application in Current Diabetes Management Practices. *Nanomaterials (Basel)* **2023**, *13* (5), 867.

(2) Alshahrani, S.; et al. Effect of thymoquinone on high fat diet and STZ-induced experimental type 2 diabetes: A mechanistic insight by in vivo and in silico studies. *J. Food Biochem* **2021**, *45*, No. e13807.

(3) Wild, S.; et al. Global prevalence of diabetes: estimates for the year 2000 and projections for 2030. *Diabetes Care* **2004**, *27* (5), 1047−53.

(4) Shoaib, A.; et al. Antidiabetic activity of standardized dried tubers extract of Aconitum napellus in streptozotocin-induced diabetic rats. *3 Biotech* **2020**, *10* (2), 56.

(5) Al-Nozha, M. M.; et al. Coronary artery disease in Saudi Arabia. *Saudi Med. J.* **2004**, *25* (9), 1165−71.

(6) Al-Hazzaa, H. M. Physical activity, fitness and fatness among Saudi children and adolescents: implications for cardiovascular health. *Saudi Med. J.* **2002**, *23* (2), 144−50.

(7) Alwan, A.d. Noncommunicable diseases: a major challenge to public health in the Region. *EMHJ-Eastern Mediterranean Health Journal* **1997**, *3* (1), 6−16. 1997.

(8) Saadia, Z.; et al. A study of knowledge attitude and practices of Saudi women towards diabetes mellitus. A (KAP) study in Al-Qassim region. *The Internet Journal of Health* **2010**, *11* (2), 1−7.

(9) Hossain, P.; Kawar, B.; Nahas, M. El Obesity and diabetes in the developing world—a growing challenge. *New England journal of medicine* **2007**, *356* (3), 213−215.

(10) Haslam, D. W.; James, W. P. T. Life expectancy. *Lancet* **2005**, *366*, 1197−1209.

(11) Hirabara, S. M. Molecular targets related to inflammation and insulin resistance and potential interventions. *BioMed. Research International* **2012**, *2012*, 1.

(12) Blagosklonny, M. TOR-centric view on insulin resistance and diabetic complications: perspective for endocrinologists and gerontologists. *Cell death & disease* **2013**, *4* (12), e964−e964.

(13) Bazotte, R. B.; Silva, L. G.; Schiavon, F. P. Insulin resistance in the liver: deficiency or excess of insulin? *Cell Cycle* **2014**, *13* (16), 2494−2500.

(14) Jung, U. J.; Choi, M.-S. Obesity and its metabolic complications: the role of adipokines and the relationship between obesity, inflammation, insulin resistance, dyslipidemia and non-alcoholic fatty liver disease. *International journal of molecular sciences* **2014**, *15* (4), 6184−6223.

(15) Santoleri, D.; Titchenell, P. M. Resolving the paradox of hepatic insulin resistance. *Cellular and molecular gastroenterology and hepatology* **2019**, *7* (2), 447−456.
(16) Guerra, S.; Gastaldelli, A. The role of the liver in the modulation of glucose and insulin in non alcoholic fatty liver disease and type 2 diabetes. *Current opinion in pharmacology* **2020**, *55*, 165−174.
(17) Loria, P.; Lonardo, A.; Anania, F. Liver and diabetes. *A vicious circle. Hepatology research* **2013**, *43* (1), 51−64.
(18) Brown, M. S.; Goldstein, J. L. Selective versus total insulin resistance: a pathogenic paradox. *Cell metabolism* **2008**, *7* (2), 95−96.
(19) James, O. F.; Day, C. P. Non-alcoholic steatohepatitis (NASH): a disease of emerging identity and importance. *Journal of hepatology* **1998**, *29* (3), 495−501.
(20) Brockmann, H. Die konstitution des alkannins, shikonins und alkannans. *Justus Liebigs Annalen der Chemie* **1936**, *521* (1), 1−47.
(21) SHOAIB, A.; et al. *Physicochemical, phytochemical and high-performance thin layer chromatography analysis of the root barks of Onosma echioides.* Asian J Pharm. *Clin Res.* **2017**, *10* (10), 196−199.
(22) Shaheen, M.; et al. Effects of different mating strategies on productive performance, bird welfare and economic appraisal of broiler breeder under two production systems. *Brazilian Journal of Poultry Science* **2020**, *22*, 22.
(23) Yannai, S. *Dictionary of food compounds with CD-ROM*; CRC Press, 2012.
(24) Papageorgiou, V. P.; et al. The chemistry and biology of alkannin, shikonin, and related naphthazarin natural products. *Angew. Chem., Int. Ed.* **1999**, *38* (3), 270−301.
(25) Saeed, M.; et al. Investigation of antidiabetic properties of shikonin by targeting aldose reductase enzyme: In silico and in vitro studies. *Biomedicine & Pharmacotherapy* **2022**, *150*, 112985.
(26) Saeed, M.; et al. Assessment of antidiabetic activity of the shikonin by allosteric inhibition of protein-tyrosine phosphatase 1B (PTP1B) using state of art: an in silico and in vitro tactics. *Molecules* **2021**, *26* (13), 3996.
(27) Munazzah, T.; et al. Computational analysis of PTP-1B site-directed mutations and their structural binding to potential inhibitors. *Cellular and Molecular Biology* **2022**, *68* (7), 75−84.
(28) Saeed, M.; et al. Identification of putative plant-based ALR-2 inhibitors to treat diabetic peripheral neuropathy. *Current Issues in Molecular Biology* **2022**, *44* (7), 2825−2841.
(29) Hosoi, T.; et al. Alkannin Attenuates Amyloid beta Aggregation and Alzheimer's Disease Pathology. *Mol. Pharmacol.* **2023**, *103* (5), 266−273.
(30) Tasleem, M.; et al. Investigation of Antidepressant Properties of Yohimbine by Employing Structure-Based Computational Assessments. *Curr. Issues Mol. Biol.* **2021**, *43* (3), 1805−1827.
(31) Alshahrani, M. Y.; et al. Computational Screening of Natural Compounds for Identification of Potential Anti-Cancer Agents Targeting MCM7 Protein. *Molecules* **2021**, *26* (19), 5878.
(32) Puius, Y. A.; et al. Identification of a second aryl phosphate-binding site in protein-tyrosine phosphatase 1B: a paradigm for inhibitor design. *Proc. Natl. Acad. Sci. U. S. A.* **1997**, *94* (25), 13420−5.
(33) Zhang, L.; et al. Inhibitor selectivity between aldo-keto reductase superfamily members AKR1B10 and AKR1B1: role of Trp112 (Trp111). *FEBS Lett.* **2013**, *587* (22), 3681−6.
(34) Bharadwaj, S.; et al. Structure-based screening and validation of bioactive compounds as Zika virus methyltransferase (MTase) inhibitors through first-principle density functional theory, classical molecular simulation and QM/MM affinity estimation. *J. Biomol Struct Dyn* **2021**, *39* (7), 2338−2351.
(35) Mena-Ulecia, K.; Tiznado, W.; Caballero, J. Study of the Differential Activity of Thrombin Inhibitors Using Docking, QSAR, Molecular Dynamics, and MM-GBSA. *PLoS One* **2015**, *10* (11), No. e0142774.
(36) *Release S4: Desmond molecular dynamics system*. DE Shaw Research, New York, NY, 2017.
(37) Kumar, G. S.; Page, R.; Peti, W. The mode of action of the Protein tyrosine phosphatase 1B inhibitor Ertiprotafib. *PLoS One* **2020**, *15* (10), No. e0240044.
(38) Kim, T. H. Aldose reductase inhibitory activity of compounds from Zea mays L. *BioMed. Research International* **2013**, *2013*, 1.
(39) Xu, F.; et al. Glucose Uptake Activities of Bis (2, 3-Dibromo-4, 5-Dihydroxybenzyl) Ether, a Novel Marine Natural Product from Red Alga Odonthaliacorymbifera with Protein Tyrosine Phosphatase 1B Inhibition, In Vitro and In Vivo. *PLoS One* **2016**, *11* (1), No. e0147748.
(40) Liu, Z. Q.; et al. Fumosorinone, a novel PTP1B inhibitor, activates insulin signaling in insulin-resistance HepG2 cells and shows anti-diabetic effect in diabetic KKAy mice. *Toxicol. Appl. Pharmacol.* **2015**, *285* (1), 61−70.
(41) Paudel, P. Protein Tyrosine Phosphatase 1B Inhibition and Glucose Uptake Potentials of Mulberrofuran G, Albanol B, and Kuwanon G from Root Bark of Morus alba L. in Insulin-Resistant HepG2 Cells: An In Vitro and In Silico Study. *Int. J. Mol. Sci.* **2018**, *19* (5), 1542.
(42) Jung, D. W.; et al. Novel use of fluorescent glucose analogues to identify a new class of triazine-based insulin mimetics possessing useful secondary effects. *Mol. Biosyst* **2011**, *7* (2), 346−58.
(43) Zhang, W. Y.; et al. 7-O-methylaromadendrin stimulates glucose uptake and improves insulin resistance in vitro. *Biol. Pharm. Bull.* **2010**, *33* (9), 1494−9.
(44) Itoh, Y.; et al. N+-C-H···O Hydrogen bonds in protein-ligand complexes. *Sci. Rep.* **2019**, *9* (1), 767.
(45) Koren, S.; Fantus, I. G. Inhibition of the protein tyrosine phosphatase PTP1B: potential therapy for obesity, insulin resistance and type-2 diabetes mellitus. *Best Pract Res. Clin Endocrinol Metab* **2007**, *21* (4), 621−40.
(46) Paudel, P.; et al. Protein tyrosine phosphatase 1B inhibition and glucose uptake potentials of mulberrofuran G, albanol B, and kuwanon G from root bark of Morus alba L. in insulin-resistant HepG2 cells: An in vitro and in silico study. *International journal of molecular sciences* **2018**, *19* (5), 1542.
(47) Sharma, B.; et al. Recent advance on PTP1B inhibitors and their biomedical applications. *Eur. J. Med. Chem.* **2020**, *199*, 112376.
(48) Hopkins, A. L.; et al. The role of ligand efficiency metrics in drug discovery. *Nat. Rev. Drug Discovery* **2014**, *13* (2), 105−121.
(49) Agoni, C.; et al. Druggability and drug-likeness concepts in drug design: are biomodelling and predictive tools having their say? *J. Mol. Model.* **2020**, *26* (6), 120.
(50) Ferreira, L. G.; et al. Molecular docking and structure-based drug design strategies. *Molecules* **2015**, *20* (7), 13384−421.
(51) Baker, E. Hydrogen bonding in biological macromolecules. *International Tables for Crystallography Volume F: Crystallography of biological macromolecules*; Springer, 2012.
(52) Saeed, M.; et al. Investigation of antidiabetic properties of shikonin by targeting aldose reductase enzyme: In silico and in vitro studies. *Biomedicine & Pharmacotherapy* **2022**, *150*, 112985.
(53) Badar, M. *Molecular Dynamics Simulations: Concept, Methods, and Applications*; Springer, 2020.
(54) Hu, X.; et al. Triterpenoid saponins from Stauntonia chinensis ameliorate insulin resistance via the AMP-activated protein kinase and IR/IRS-1/PI3K/Akt pathways in insulin-resistant HepG2 cells. *Int. J. Mol. Sci.* **2014**, *15* (6), 10446−58.
(55) Cordero-Herrera, I.; et al. Cocoa flavonoids attenuate high glucose-induced insulin signalling blockade and modulate glucose uptake and production in human HepG2 cells. *Food Chem. Toxicol.* **2014**, *64*, 10−9.
(56) Haraguchi, H.; Ohmi, I.; Kubo, I. Inhibition of aldose reductase by maesanin and related p-benzoquinone derivatives and effects on other enzymes. *Bioorg. Med. Chem.* **1996**, *4* (1), 49−53.
(57) Demir, Y. Phenolic compounds inhibit the aldose reductase enzyme from the sheep kidney. *J. Biochem Mol. Toxicol* **2017**, *31* (9), e21936.

https://doi.org/10.1021/acsomega.4c00082
ACS Omega 2024, 9, 36099−36113

(58) Patil, K. K.; Gacche, R. N. Inhibition of glycation and aldose reductase activity using dietary flavonoids: A lens organ culture studies. *Int. J. Biol. Macromol.* **2017**, *98*, 730−738.
(59) Du, Z. Y.; et al. Curcumin analogs as potent aldose reductase inhibitors. *Arch Pharm. (Weinheim)* **2006**, *339* (3), 123−8.
(60) Muthenna, P.; et al. Inhibition of aldose reductase by dietary antioxidant curcumin: mechanism of inhibition, specificity and significance. *FEBS Lett.* **2009**, *583* (22), 3637−42.
(61) Varma, S. D.; Mizuno, A.; Kinoshita, J. H. Diabetic cataracts and flavonoids. *Science* **1977**, *195* (4274), 205−6.
(62) Chaudhry, P. S.; et al. Inhibition of human lens aldose reductase by flavonoids, sulindac and indomethacin. *Biochem. Pharmacol.* **1983**, *32* (13), 1995−8.
(63) Veverka, M.; et al. Novel quercetin derivatives: synthesis and screening for anti-oxidant activity and aldose reductase inhibition. *Chemical Papers* **2013**, *67* (1), 76−83.
(64) Ahn, J. H.; et al. Synthesis and PTP1B inhibition of 1,2-naphthoquinone derivatives as potent anti-diabetic agents. *Bioorg. Med. Chem. Lett.* **2002**, *12* (15), 1941−6.
(65) Zhao, B. T.; et al. Protein tyrosine phosphatase 1B inhibitors from natural sources. *Arch Pharm. Res.* **2018**, *41* (2), 130−161.
(66) Nurul Islam, M.; et al. Potent alpha-glucosidase and protein tyrosine phosphatase 1B inhibitors from Artemisia capillaris. *Arch Pharm. Res.* **2013**, *36* (5), 542−52.
(67) Ali, M. Y.; et al. Coumarins from Angelica decursiva inhibit alpha-glucosidase activity and protein tyrosine phosphatase 1B. *Chem. Biol. Interact* **2016**, *252*, 93−101.
(68) Jeong, S. Y.; et al. Chemical Constituents of Euonymus alatus (Thunb.) Sieb. and Their PTP1B and alpha-Glucosidase Inhibitory Activities. *Phytother Res.* **2015**, *29* (10), 1540−8.
(69) Chen, R. M.; et al. Natural PTP1B inhibitors from Broussonetia papyrifera. *Bioorg. Med. Chem. Lett.* **2002**, *12* (23), 3387−90.
(70) Zhang, J.; et al. Phenolic compounds from the leaves of Cyclocarya paliurus (Batal.) Ijinskaja and their inhibitory activity against PTP1B. *Food Chem.* **2010**, *119* (4), 1491−1496.
(71) Cai, J.; Zhao, L.; Tao, W. Potent protein tyrosine phosphatase 1B (PTP1B) inhibiting constituents from Anoectochilus chapaensis and molecular docking studies. *Pharm. Biol.* **2015**, *53* (7), 1030−4.
(72) Guo, Z.; et al. Chemical profile and inhibition of α-glycosidase and protein tyrosine phosphatase 1B (PTP1B) activities by flavonoids from licorice (Glycyrrhiza uralensis Fisch). *Journal of Functional Foods* **2015**, *14*, 324−336.
(73) Na, B.; et al. Protein tyrosine phosphatase 1B (PTP1B) inhibitory activity and glucosidase inhibitory activity of compounds isolated from Agrimonia pilosa. *Pharm. Biol.* **2016**, *54* (3), 474−80.
(74) Zhao, B. T.; et al. PTP1B, alpha-glucosidase, and DPP-IV inhibitory effects for chromene derivatives from the leaves of Smilax china L. *Chem. Biol. Interact* **2016**, *253*, 27−37.
(75) Na, M.; et al. Protein tyrosine phosphatase-1B inhibitory activity of isoprenylated flavonoids isolated from Erythrina mildbraedii. *J. Nat. Prod* **2006**, *69* (11), 1572−6.
(76) Cui, L.; et al. New prenylated flavanones from Erythrina abyssinica with protein tyrosine phosphatase 1B (PTP1B) inhibitory activity. *Planta Med.* **2010**, *76* (7), 713−8.
(77) Nguyen, P. H.; et al. New 5-deoxyflavonoids and their inhibitory effects on protein tyrosine phosphatase 1B (PTP1B) activity. *Bioorg. Med. Chem.* **2011**, *19* (11), 3378−83.
(78) Nguyen, P. H.; et al. New prenylated isoflavonoids as protein tyrosine phosphatase 1B (PTP1B) inhibitors from Erythrina addisoniae. *Bioorg. Med. Chem.* **2012**, *20* (21), 6459−64.
(79) Sasaki, T.; et al. Protein tyrosine phosphatase 1B inhibitory activity of lavandulyl flavonoids from roots of Sophora flavescens. *Planta Med.* **2014**, *80* (7), 557−60.
(80) Wu, L. Q.; et al. Isoprenylated Flavonoids with PTP1B Inhibition from Ficus tikoua. *Nat. Prod Commun.* **2015**, *10* (12), 2105−7.
(81) Wang, Y.; et al. Novel chromenedione derivatives displaying inhibition of protein tyrosine phosphatase 1B (PTP1B) from Flemingia philippinensis. *Bioorg. Med. Chem. Lett.* **2016**, *26* (2), 318−321.
(82) Jung, H. A.; et al. Prunin is a highly potent flavonoid from Prunus davidiana stems that inhibits protein tyrosine phosphatase 1B and stimulates glucose uptake in insulin-resistant HepG2 cells. *Arch Pharm. Res.* **2017**, *40* (1), 37−48.
(83) Li, W.; et al. Evaluation of licorice flavonoids as protein tyrosine phosphatase 1B inhibitors. *Bioorg. Med. Chem. Lett.* **2013**, *23* (21), 5836−9.
(84) Hoang, D. M.; et al. Protein tyrosine phosphatase 1B inhibitors isolated from Morus bombycis. *Bioorg. Med. Chem. Lett.* **2009**, *19* (23), 6759−61.
(85) Yoon, G.; et al. Inhibitory effect of chalcones and their derivatives from Glycyrrhiza inflata on protein tyrosine phosphatase 1B. *Bioorg. Med. Chem. Lett.* **2009**, *19* (17), 5155−7.

https://doi.org/10.1021/acsomega.4c00082
ACS Omega 2024, 9, 36099−36113